Structural Effects on Intermolecular Electron Transfer Reactivity

Stephen F. Nelsen,*,† Dwight A. Trieber, II,† Mark A. Nagy,† Asgeir Konradsson,† DeWayne T. Halfen,‡ Kathryn A. Splan,‡ and Jack R. Pladziewicz*,‡

Contribution from the Department of Chemistry, University of Wisconsin, Madison, Wisconsin 53706-1396, and the Department of Chemistry, University of Wisconsin, Eau Claire, Wisconsin 54702-4004

Received October 4, 1999

Abstract: Rate constants (k_{ij}) measured by stopped flow are reported for 50 additional intermolecular electron transfer reactions between 0 and 1+ oxidation states of various compounds, enlarging our data set to 141 reactions between 45 couples in acetonitrile containing 0.1 M tetrabutylammonium perchlorate at 25 °C. Hydrazines with both saturated and unsaturated substituents, ferrocene derivatives, and heteroatom-substituted aromatic compounds are included in the couples studied. Least-squares fit of all the reactions to simple Marcus cross-reaction theory provides an internally consistent set of best fit intrinsic barriers $\Delta G^{\ddagger}_{ii}$(fit) (for self-electron transfer of each couple) covering a range of over 19 kcal/mol (rate constant range 2×10^{14}) that predicts the k_{ij} rather accurately. All reactions have ratios of calculated to observed k_{ij} in the range 0.3−3.3 and 95% fall in the range 0.5−2.0. These results require that the preexponential factor for a cross reaction is close to the geometric mean of those for the self-reactions, which is not expected. Changes in internal reorganization energy (λ_v) have major effects on $\Delta G^{\ddagger}_{ii}$(fit), and changes in electronic overlap (H_{ab}) have easily detectable ones, but the reactions studied are clearly not strongly nonadiabatic, even though in many cases the only electronic overlap at the transition state is between nonbonded alkyl groups. It is argued that these reactions occur in the "elbow region" between nonadiabatic and adiabatic electron transfer.

Introduction

Outer-sphere single electron transfer (ET) reactions between a neutral species $\mathbf{i^0}$, and a radical cation, $\mathbf{j^+}$, eq 1, are the simplest cases for calculation of rate constants. Marcus introduced the

$$\mathbf{i^0} + \mathbf{j^+} \rightarrow \mathbf{i^+} + \mathbf{j^0} \tag{1}$$

concept that the rate constant k_{ij} for eq 1 could be calculated from the intrinsic reactivities of the couples involved, the self-exchange rate constants k_{ii} and k_{jj} at zero driving force, and the thermodynamics for ET between the couples. The thermodynamics for the reaction are usually available from electrochemistry when the couples are stable enough that k_{ij} can be experimentally measured. Because one component has zero charge, corrections for electrostatic work terms are not required, simplifying Marcus's cross-reaction relations to eq 2.[1]

$$k_{ij}(\text{calcd}) = (k_{ii}k_{jj}K_{ij}\,f_{ij})^{1/2} \tag{2a}$$

$$\ln(f_{ij}) = [\ln(K_{ij})]^2/[4\,\ln(k_{ii}k_{jj}/Z^2)] \tag{2b}$$

K_{ij} is the equilibrium constant for eq 1, and Z is the preexponential factor. The more general form of eq 2, including work terms, has been successfully applied to a wide variety of inorganic, organic, organometallic, and biochemical reactions.[2−4] However, modern ET theory indicates that eq 2 will not suffice. Equation 2 was derived assuming that ET reactions are adiabatic, which requires the preexponential factor to be constant and the rate constant to be controlled by the activation barrier. The fundamental assumption producing eq 2 was that averaging the activation barriers for self-exchange reactions produced the proper activation barrier for the cross reactions. In the latest review on ET chemistry, Bixon and Jorter say that although there was "lively discussion" in the 1960s about whether ET reactions were adiabatic or nonadiabatic, it has now been established that the great majority are nonadiabatic (ref 5, p 52). If this is the case, eq 2 should not work, because nonadiabatic reaction rate constants are controlled not only by activation barriers but by widely varying preexponential factors. In addition to the vertical reorganization energy (λ) that controls the rate constant for adiabatic ET, the size of the electronic interaction between the partners at the ET transition state (also called the electronic coupling matrix element, H_{ab}) and the energy corresponding to the inherent barrier-crossing frequency ($\tilde{\nu}_v$) are important in determining the rate constant for nonadiabatic reactions. We showed that despite predictions of modern theory, eq 2 successfully correlates cross rate data for couples having a wide range of structural types, including heteratom-substituted aromatics, methylated ferrocenes, many tetraalkylhydrazines, and Alder's triply trimethylene-bridged diamine.[6] Best fit to eq 2 for 91 reactions studied between

† University of Wisconsin, Madison.

‡ University of Wisconsin, Eau Claire.

(1) (a) Marcus, R. A. *J. Chem. Phys.* **1956**, *24*, 966. (b) Marcus, R. A. *Discuss. Faraday Soc.* **1960**, *29*, 21. (c) Marcus, R. A. *J. Phys. Chem.* **1963**, *67*, 853, 2889. (d) Marcus, R. A.; Sutin, N. *Inorg. Chem.* **1975**, *14*, 213.

(2) (a) Marcus, R. A.; Sutin, N. *Biochim. Biophys. Acta* **1985**, *811*, 265. (b) Sutin, N. *Prog. Inorg. Chem.* **1983**, *30*, 441.

(3) Wherland, S. *Coord. Chem. Rev.* **1993**, *123*, 169−99.

(4) Eberson, L. *Electron-Transfer Reactions in Organic Chemistry*; Springer-Verlag: Heidelberg, 1987.

(5) Bixon, M.; Jortner, J. *Adv. Chem. Phys.* **1999**, *106*, 35−202.

(6) (a) Nelsen, S. F.; Wang, Y.; Ramm, M. T.; Accola, M. A.; Pladziewicz, J. R. *J. Phys. Chem.* **1992**, *96*, 10654. (b) Nelsen, S. F.; Chen, L.-J.; Ramm, M. T.; Voy, G. T.; Powell, D. R.; Accola, M. A.; Seehafer, T.; Sabelko, J.; Pladziewicz; J. R. *J. Org. Chem.* **1996**, *61*, 1405. (c) Nelsen, S. F.; Ismagilov, R. F.; Chen, L.-J.; Brandt, J. L.; Chen, X.; Pladziewicz, J. R. *J. Am. Chem. Soc.* **1996**, *118*, 1555. (d) Nelsen, S. F.; Ramm, M. T.; Ismagilov, R. F.; Nagy, M. A.; Trieber, D. A., II; Powell, D. R.; Chen, X.; Gengler, J. J.; Qu, Q.; Brandt, J. L.; Pladziewicz, J. R. *J. Am. Chem. Soc.* **1997**, *119*, 5900. (e) Nelsen, S. F.; Ismagilov, R. F.; Gentile, K. E.; Nagy, M. A.; Tran, H. Q.; Qu, Q.; Halfen, D. T.; Oldegard, A. L.; Pladziewicz, J. R. *J. Am. Chem. Soc.* **1998**, *120*, 8230.

10.1021/ja993573o CCC: $19.00
Published on Web 06/10/2000

Scheme 1. Couples First Studied in This Work

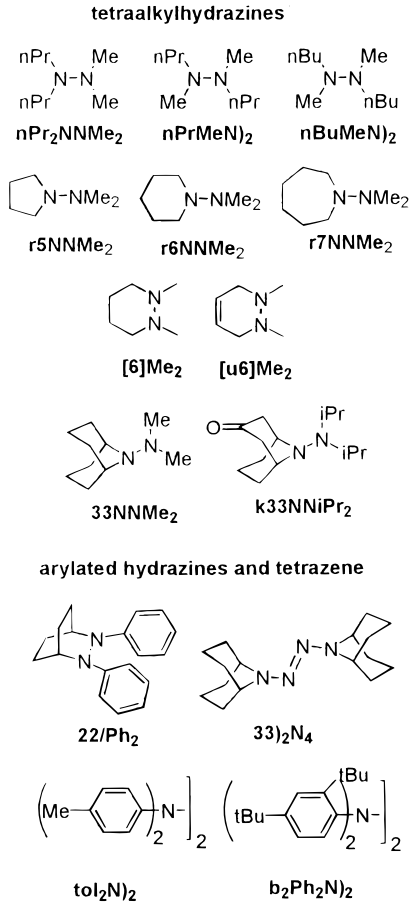

31 compounds gave k_{ii}(fit) values producing k_{ij}(calcd) values having k_{ij}(obsd)/k_{ij}(calcd) in the range 0.5 to 2.0. The fitted self-exchange activation barriers $\Delta G^{\ddagger}_{ii}$(fit) ranged from 2.3 kcal/mol for tetramethyltetraselenafulvalene to 21.8 kcal/mol for tetra-*n*-propylhydrazine, corresponding to a huge range in k_{ii}(fit), a factor of 2×10^{14}. In this work we report rate constants for additional cross-reactions, and return to the questions of what factors really are important for determining intermolecular ET reactivity, and what eq 2 working so well implies.

Results

Fifty additional reactions employing ten additional tetraalkylhydrazines, three hydrazines having aryl substituents, and the first 2-tetrazene examined are reported here (see Scheme 1 for the structures). Scheme 2 shows the structures of 14 couples that were extensively used as partners in determining observed rate constants in this work, while Scheme 3 shows the 17 additional couples in the data set that were either not used or only used for one reaction. This work expands our data set to 141 reactions studied under the same conditions, 298 K in acetonitrile containing 0.1 M tetrabutylammonium perchlorate. Data acquisition and analysis were as reported previously.[6] The primary information available from the analysis of cross rate studies is the k_{ii}(fit) value for each couple, which we converted to the free energy barrier $\Delta G^{\ddagger}_{ii}$(fit) using the Eyring rate expression, eq 3, constants shown for 25 °C, and $\Delta G^{\ddagger}$ in kcal/

$$k = (k_B T/h) \exp(-\Delta G^{\ddagger}/RT) = (6.21 \times 10^{12}) \exp(-\Delta G^{\ddagger}/0.592) \quad (3)$$

mol. The $\Delta G^{\ddagger}_{ii}$(fit) values are linearly related, and allow direct comparison of intrinsic reactivities. The fitted intrinsic reactivity

Scheme 2. Couples Principally Used to Measure k_{ij} Values for the Scheme 1 Couples

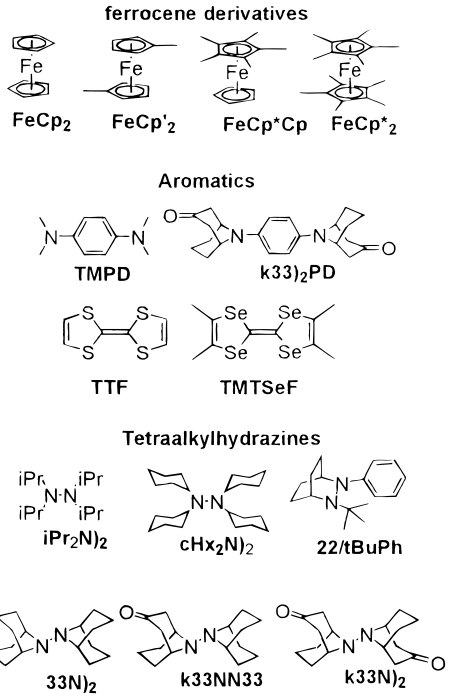

Scheme 3. Additional Previously Studied Couples Studied

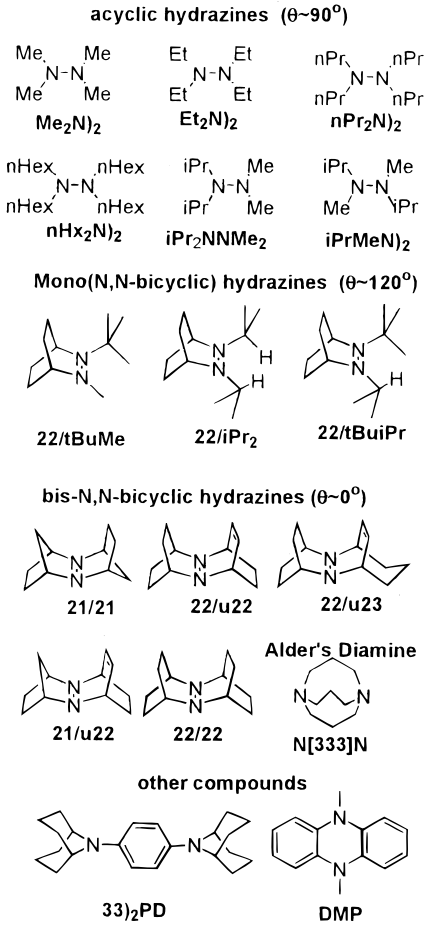

data for the compounds of Schemes 1 and 2 are summarized in Table 1; these data for the compounds of Scheme 3 appear in the Supporting Information, as do the observed and fitted cross rate constants, for all 50 reactions studied here.

Table 1. Instrinsic Reactivity Data for the Couples of Schemes 1 and 2 (141 reaction set)

redox couple	$E^{\circ\prime}$ (V)	no. of reactions[a]	k_{ii}(fit) ($M^{-1}\,s^{-1}$)	$\Delta G^{\ddagger}_{ii}$(fit) (kcal/mol)[a]
acyclic hydrazines				
$(^{i}Pr_2N)_2^{0/+}$	0.26	21 (14)	3.2×10^{-3}	20.9 (21.0)
$(cHx_2N)_2^{0/+}$	0.26	20 (13)	2.5×10^{-2}	19.6 (19.7)
$^{n}Pr_2NNMe_2^{0/+}$	0.30	4	4.2×10^{-2}	19.3
$(^{n}PrMeN)_2^{0/+}$	0.30	3	4.4×10^{-2}	19.3
$(^{n}BuMeN)_2^{0/+}$	0.29	4	4.9×10^{-2}	19.2
monocyclic hydrazines				
$r7NNMe_2^{0/+}$	0.23	3	3.0×10^{-1}	18.2
$[u6]Me_2^{0/+}$	0.33	3	1.2×10^{0}	17.4
$r6NNMe_2^{0/+}$	0.36	2	3.1×10^{0}	16.8
$r5NNMe_2^{0/+}$	0.17	3	3.9×10^{0}	16.6
$[6]Me_2^{0/+}$	0.23	2	5.2×10^{1}	15.1
9-azabicyclononyl hydrazines				
$k33NNiPr_2^{0/+}$	0.29	5	5.6×10^{-2}	19.2
$(k33N)_2^{0/+}$	0.45	14 (7)	3.1×10^{1}	15.4 (15.3)
$k33NN33^{0/+}$	0.22	12 (8)	2.5×10^{2}	14.2 (14.2)
$(33N)_2^{0/+}$	−0.01	11 (8)	7.3×10^{2}	13.5 (13.6)
$33NNMe_2^{0/+}$	0.11	4	7.2×10^{2}	13.5
aryl-substituted hydrazines				
$22/^{t}BuPh^{0/+}$	0.26	8 (5)[b]	1.0×10^{3}	13.3 (13.4)[b]
$22/Ph_2^{0/+}$	0.48	7	5.6×10^{4}	11.0
$(b_2Ph_2N)_2^{0/+}$	0.61	5	5.6×10^{6}	8.2
$(tol_2N)_2^{0/+}$	0.65	3	8.1×10^{8}	5.3
2-tetrazene				
$(33)_2N_4^{0/+}$	0.40	7	4.4×10^{5}	9.8
ferrocene derivatives				
$FeCp^*_2^{0/+}$	−0.11	8 (6)	9.9×10^{6}	7.9 (7.9)
$FeCp^*Cp^{0/+}$	0.12	11 (6)	8.1×10^{6}	8.0 (7.9)
$FeCp'_2^{0/+}$	0.28	3 (1)	6.4×10^{6}	8.0 (7.7)
$FeCp_2^{0/+}$	0.395	4 (1)	1.5×10^{7}	7.7 (8.1)
aromatic compounds				
$(k33)_2PD^{0/+}$	0.29	18 (3)	3.1×10^{7}	7.2 (7.1)
$TMPD^{0/+}$	0.12	8 (4)	1.1×10^{8}	6.5 (6.4)
$TTF^{0/+}$	0.33	13 (9)[b]	1.2×10^{10}	3.7 (4.1)[b]
$TMTSF^{0/+}$	0.42	13 (8)[b]	1.2×10^{11}	2.3 (2.3)[b]

[a] The numbers in parentheses, unless otherwise indicated, are from the 47 reaction data set of ref 5d. [b] Numbers in parentheses are from the 91 reaction data set of ref 5e.

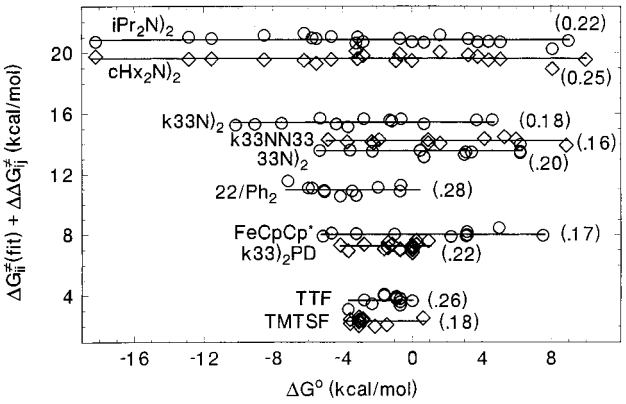

Figure 1. Plot of $\Delta G^{\ddagger}_{ii}$(fit) plus the deviation of observed and calculated $\Delta G^{\ddagger}_{ij}$ versus the driving force for each cross reaction studied, for the 10 couples that were used most often.

The sort of scatter in intrinsic reactivity observed from reaction to reaction seems best considered using the graphical display shown in Figure 1 for the 10 most-used couples (21 to 10 reactions). The vertical axis is the sum of $\Delta\Delta G^{\ddagger}_{ij}$(obsvd − calcd) and $\Delta G^{\ddagger}_{ii}$(fit), and the horizontal axis is ΔG° (kcal/mol) for each reaction, shown as $23.06(E^{\circ\prime}$(couple shown) − E'(partner)), so a negative number results when the radical cation of the couple shown was used in an exoergonic reaction with a neutral partner. The plot shows the relative internal agreement of individual $\Delta G^{\ddagger}_{ii}$(fit) and the extent to which each individual reaction used to compute it differs from the mean. It also shows the expected independence of $\Delta G^{\ddagger}_{ii}$(fit) on ΔG°_{ij}. The root-mean-square deviation for each couple is shown in parentheses at the right of Figure 1. The average $|\Delta\Delta G^{\ddagger}_{ij}|$, the deviation of observed from calculated activation barrier, increased from 0.13 kcal/mol for the 91 reaction set to 0.18 kcal/mol for the 141 reaction set. Agreement between k_{ij}(obsd) and k_{ij}(calcd) using eq 2 remains excellent. One hundred and thirty four of the reactions (95%) have $|\Delta\Delta G^{\ddagger}_{ij}| \leq 0.41$ kcal/mol (k_{ij}(obsd)/k_{ij}(calcd) in the range 0.5 to 2.0). Poorest agreement is shown for reactions 94, 95, 125, 133, and 141, which have k_{ij}(obsd)/k_{ij}(calcd) in the range 2.08−3.27 ($\Delta\Delta G^{\ddagger}_{ij}$ in the range −0.43 to −0.70 kcal/mol), and 124 and 140, rate ratios 0.38 and 0.28 ($\Delta\Delta G^{\ddagger}_{ij}$ in the range 0.57 to 0.76 kcal/mol), see the Supporting Information for details. Five of these seven reactions showing the largest deviations involve the especially hindered aromatic hydrazines $\mathbf{22/Ph_2}$ and $\mathbf{(b_2Ph_2N)_2}$.

Discussion

Structural Effects on Intrinsic Reactivity. Our studies show that knowing only the formal oxidation potential and an intrinsic rate constant for each couple suffices to calculate k_{ij} for cross reactions of the couple with other couples having a wide range of structure and reactivity. Although predicted in 1956 by Marcus, this result is rather surprising in terms of modern ET theory: it is clear that the reactions studied are not adiabatic, yet eq 2 still works to a surprising degree of accuracy. Cross-reaction studies considerably extend the range of structural variation available for comparing intrinsic reactivities over that from self-exchange studies. Very fast reactions are diffusion limited instead of activation limited under self-exchange conditions, precluding obtaining $\Delta G^{\ddagger}_{ii}$ from k_{ii} self-exchange measurements. Magnetic resonance line-broadening methods fail when k_{ii} is $<\sim 5 \times 10^2\ M^{-1}\ s^{-1}$, and radical cation decomposition is faster than self-exchange for most compounds with small k_{ii} values. Cross-reaction studies also allow the same experimental method to be used for a very wide range of couples and only require that the cation be stable under the reaction conditions for the time it takes to record data (typically less than a second). They also clearly indicate if stability is insufficient, because single exponential pseudo-first-order decays are not obtained when decomposition is significant. Intrinsic barriers for over half of the couples studied can only be determined under cross-reaction conditions.

The $\Delta G^{\ddagger}_{ii}$(fit) values clearly correlate with structure, as shown graphically in Figure 2. Tetraalkylhydrazines are by far the least reactive compounds studied, ferrocenes are somewhat less reactive than aromatic compounds, and among the aromatic compounds, amino-substituted ones are less reactive than tetrathiafulvalene (**TTF**) and tetramethyltetraselenafulvalene (**TMTSF**). There is a huge range of reactivity for hydrazines, and the two tetraarylhydrazines studied span the $\Delta G^{\ddagger}_{ii}$(fit) range for amino-substituted aromatics. $\Delta G^{\ddagger}_{ii}$(fit) values correlate well with $\Delta G^{\ddagger}_{ii}$ values that have been measured directly under self-exchange conditions, although $\Delta G^{\ddagger}_{ii}$(fit) is systematically slightly higher than $\Delta G^{\ddagger}_{ii}$(self).[6d] It seems plausible that intermolecular electronic interaction (H_{ab}) might be slightly larger for a self-exchange reaction than for a cross reaction because of better orbital energy level matching for the self-exchange.[6d] The largest deviation in terms of fraction of the barrier (fraction 0.31, 1.5 kcal/mol) is found for the unhindered

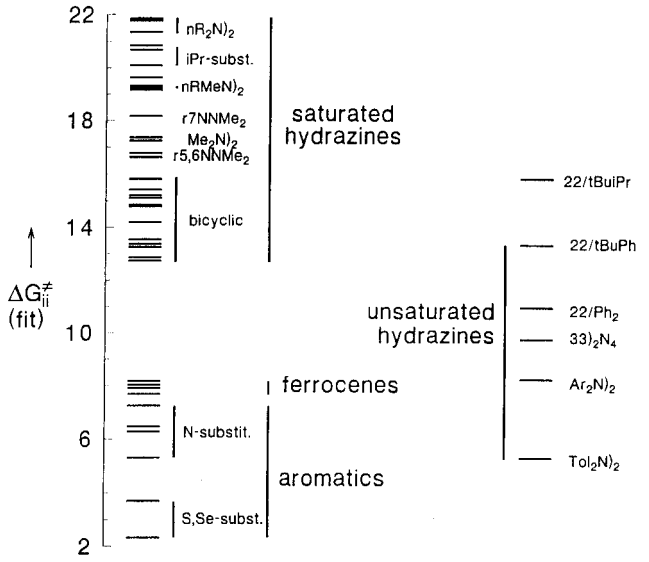

Figure 2. Comparison of $\Delta G^{\ddagger}_{ii}$(fit) values.

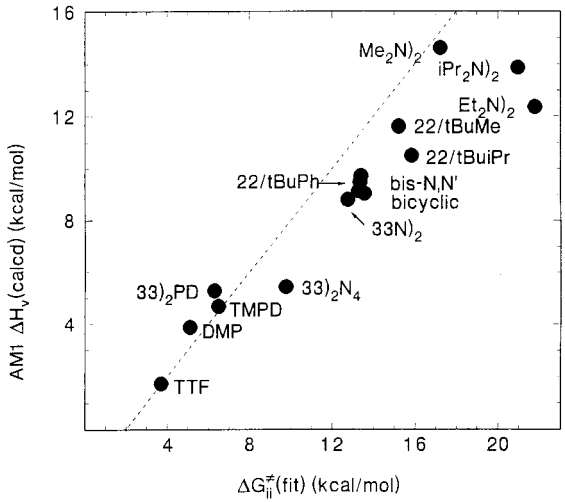

Figure 3. Plot of AM1-calculated vertical reorganization enthalpy barrier contribution ($\Delta H^{\ddagger}_v$) versus fitted free energy barrier ($\Delta G^{\ddagger}_{ii}$(fit)) for selected compounds.

and nearly planar **TMPD**$^{0/+}$, where orbital overlap between the self-exchange partners is certainly expected to be larger than for any of the cross reactions studied. Nevertheless, $\Delta G^{\ddagger}_{ii}$(fit) is also larger than $\Delta G^{\ddagger}_{ii}$(self) for all six of the very hindered bis(bicyclic) hydrazines studied,[6d,7] by an average of 0.7 kcal/mol; the effect does not only occur for the least hindered compounds.

The principal factor controlling changes in $\Delta G^{\ddagger}_{ii}$(fit) with structure is rather clearly the intramolecular vertical reorganization energy (Marcus's λ_v), and reasonable λ_v values appear to be estimated for hydrazines and some aromatic compounds using the simple AM1 method.[6e] Heats of formation for geometry-optimized structures of the relaxed neutral (**n**^{0}) and radical cation (**c**$^+$), and for the vertical cation (**n**$^+$) and neutral (**c**^{0}) give the enthalpy portion of the vertical reorganization energy using eq 4.[8] Although AM1 calculations give rather poor NN bond

$$\lambda'_v = [\Delta H_f(\mathbf{n}^+) - \Delta H_f(\mathbf{c}^+)] + [\Delta H_f(\mathbf{c}^0) - \Delta H_f(\mathbf{n}^0)] = 4\Delta H_v \quad (4)$$

lengths, they get the pyramidality at nitrogen of the radical cation more accurately than far more expensive ab initio calculations. Even using a 6-31G* basis set, which takes on the order of 10^6 longer to carry out than an AM1 calculation, produces too much flattening at nitrogen in the radical cations. Changes in the lone pair, lone pair dihedral angle θ and in the pyramidality at nitrogen between the neutral and radical cation oxidation states are the most important factors leading to differences in λ_v for different hydrazines. The first term of eq 4 ([$\Delta H_f(\mathbf{n}^+)$ − $\Delta H_f(\mathbf{c}^+)$]) is the difference between the vertical and adiabatic ionization potentials, an experimentally measurable number. AM1 calculations have been shown experimentally to be surprisingly accurate for tetraalkylhydrazines.[8] The principal problem with calculations of λ_v is that when several conformations of similar energy are present, the value obtained can be rather sensitive to which are chosen, and we do not know how to decide what conformations to use.

Because the total vertical reorganization energy is the sum of λ_v and the solvent reorganization energy λ_s, we previously tried to correct the experimental $\Delta G^{\ddagger}_{ii}$(fit) values for the $\Delta G^{\ddagger}$(solvent) component using the calculated molecular size and Marcus's equation for λ_s,[1] before comparing calculated ΔH_v with experimental data.[6e] However, this gives corrections to $\Delta G^{\ddagger}$ in the rather narrow range 2.6 ± 0.5 kcal/mol for all compounds considered here, and as argued previously, these corrections may well be overestimated. We therefore simply plot $\Delta G^{\ddagger}_{ii}$(fit) versus the AM1-calculated ΔH_v in Figure 3. The dotted line represents a linear correlation between the calculated and experimental numbers using an average $\lambda_s/4$ of 2 kcal/mol. We find it striking that AM1 calculations do such a good job of estimating intrinsic barriers for ET of so many of these compounds. Besides solvent reorganization corrections (expected to correspond to a shift of a maximum of ± 0.5 kcal/mol on the *x* axis), smaller electronic interaction between the ET partners (H_{ab}) or equilibrium constant for encounter complex formation (K_e) will move points right on the *x* axis. As considered in more detail below, significantly smaller H_{ab} occurs for hydrazines with *n*-alkyl substituents than for **(Me$_2$N)$_2$**. The AM1-calculated ΔH_v values are certainly not perfect: it seems unlikely that **(Et$_2$N)$_2$** has as much smaller a ΔH_v than **(Me$_2$N)$_2$** as we obtained (there are many more conformations available for the ethylated compounds and it is not clear we used the appropriate ones). An apparently unreasonably large ΔH_v value (8.3 kcal/mol) was obtained for **(Ph$_2$N)$_2$**, calculated as a model for the **(tol$_2$N)$_2$** studied. Although we are unable to find a minimum for twisted **(Ph$_2$N)$_2^{\bullet+}$**, the calculated ΔH_v could only be consistent with $\Delta G^{\ddagger}_{ii}$(fit) if the cation initially produced were twisted.

Discussion

Dissection of Intrinsic Reactivities into λ and H_{ab}. The $\Delta G^{\ddagger}_{ii}$(fit) values of Table 1 and Figure 2 are the intrinsic reactivities: combined with $E^{\circ\prime}$, they allow calculation of k_{ij} rather accurately. They are, however, dissatisfying because they do not address what gives rise to the intrinsic reactivity in terms of ET rate theory. As noted previously,[6] our data appear to us to require that H_{ab} affects both the exponential and preexponential terms of the rate equation. For its effect on the exponential term, we use eq 5, which arises from a classical two-state Marcus−Hush type model. For the preexponential term effect, we previously used a semiclassical two-state model

$$\Delta G^* = \lambda/4 - H_{ab} + (H_{ab})^2/\lambda \quad (5)$$

(7) (a) Nelsen, S. F.; Blackstock, S. C. *J. Am. Chem. Soc.* **1985**, *107*, 7189. (b) Nelsen, S. F.; Wang, Y. *J. Org. Chem.* **1994**, *59*, 1655.

(8) Nelsen, S. F.; Blackstock, S. C.; Kim, Y. *J. Am. Chem. Soc.* **1987**, *109*, 677.

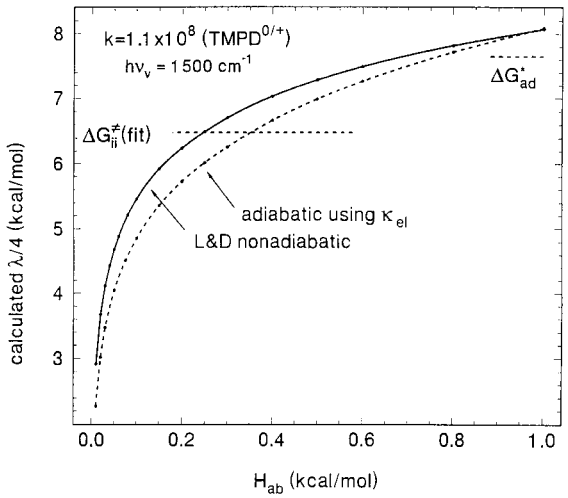

Figure 4. Comparison of $\lambda/4$ values calculated using the nonadiabatic eq 7 (solid line) and the adiabatic eq 6 (broken curve) with k_{ii}(fit) for **TMPD**$^{0/+}$, $\tilde{\nu}_v = 1500$ cm^{-1}, $T = 25$ °C.

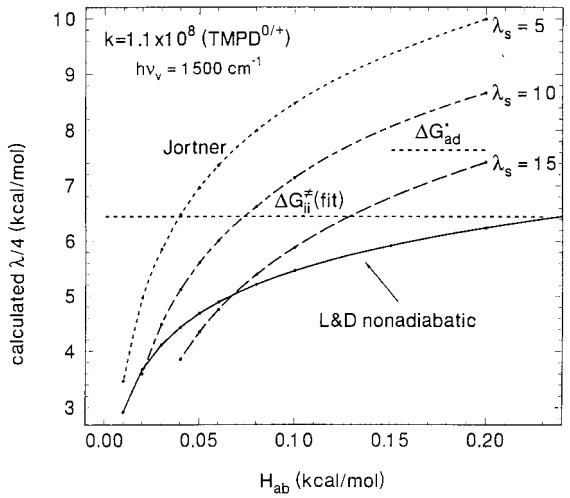

Figure 5. Comparison of $\lambda/4$ values calculated using the nonadiabatic eq 7 (solid line) and Jortner double sum vibronic coupling theory (broken curves) with k_{ii}(fit) for **TMPD**$^{0/+}$, $\tilde{\nu}_v = 1500$ cm^{-1}, $T = 25$ °C.

including a transmission coefficient κ_{el} (see eqs 6a−d) with an adiabatic preexponential factor.[2b]

$$k_{ad} = K_e \kappa_{el} \nu_v \exp(-\Delta G^*/RT) \quad (6a)$$

$$\kappa_{el} = [1 - \exp(-\nu_{el}/2\nu_v)]/[1 - {}^1/_2 \exp(-\nu_{el}/2\nu_v)] \quad (6b)$$

$$\nu_v = (2.998 \times 10^{10})\tilde{\nu}_v \quad (6c)$$

$$\nu_{el}(298\ \mathrm{K}) = (1.52 \times 10^{14})(H_{ab})^2/(\lambda)^{1/2}) \quad (6d)$$

Although frequently written without the encounter complex equilibrium constant term, K_e, it must be included to properly describe intermolecular reactions. Problems in applying eq 6 to experimental data are that there is no good way to separate λ into its solvent and vibrational components, and that $\tilde{\nu}_v$ is not usually known. Here we continue to use the conventional values of 400 cm^{-1} for ferrocenes, 800 cm^{-1} for hydrazines, and 1500 cm^{-1} for aromatic compounds. We had not previously realized how similar using eq 6 is to employing the simplest type of nonadiabatic rate equation, which we will call a Levich and Dogonadze type (L&D) expression, shown as eq 7. Although used outside the range for which it was designed, it also allows

$$k_{L\&D} = K_e(2\pi/\hbar)H_{ab}{}^2(4\pi RT\lambda)^{-1/2} \exp[-\Delta G^*/RT] \quad (7)$$

connecting the high (adiabatic) and low (nonadiabatic) H_{ab} regimes, and uses a simpler expression that avoids the use of $\tilde{\nu}_v$ or separation of λ into its components.[9] Figure 4 compares the interpretation of the $\Delta G^{\ddagger}_{ii}$(fit) measurement of **TMPD**$^{0/+}$ using $\tilde{\nu}_v = 1500$ cm^{-1}, in terms of $\lambda/4$ versus H_{ab} plots using semiclassical adiabatic (eq 6) and L&D nonadiabatic (eq 7) theory (K_e set equal to 1 for both plots). The results are similar enough that distinguishing between these theories experimentally appears unlikely. The $\lambda/4$ curve using eq 7 lies 0.65 kcal/mol higher than that using eq 6 at small H_{ab}, but the difference drops steadily as H_{ab} increases until the curves cross near 1 kcal/mol. All of the points plotted in Figure 4 correspond to the same $\Delta G^{\ddagger}_{ii}$(fit) value, emphasizing that extracting the vertical reorganization energy from a k_{ii} measurement requires knowing H_{ab}.

It is clear that the reactions studied do not lie in the strongly nonadiabatic regime, where k_{ii} must be calculated using the vibronic coupling theory expressions derived by Jortner and co-workers. In the strongly nonadiabatic region, k_{ii} is directly proportional to $H_{ab}{}^2/(\lambda^{1/2})e^{-S}$, where $S = \lambda_v/\tilde{\nu}_v$ (ref 5, p 55). Figure 5 compares $\lambda/4$ versus H_{ab} values calculated for the same system as Figure 4 using this theory (with the double sum Franck−Condon factor that is necessary for $\Delta G° = 0$ reactions).[10] Values for λ_s and λ_v must be specified to apply this theory, resulting in families of fits depending on the partitioning of λ between solvent and internal modes, as indicated by the three broken curves using $\lambda_s = 5$ (probably too small), 10, and 15 (probably too large) kcal/mol. The slopes of the plots are clearly significantly larger when the fully implemented vibronic coupling theory of Jortner and co-workers is employed instead of the L&D expression, making the intrinsic barrier even more sensitive to H_{ab} using Jortner theory. Using conventional values for $\tilde{\nu}_v$ and λ_v values of ≥ 60, ≤ 8, and ≤ 20 for hydrazines, ferrocenes, and aromatic compounds, respectively (we feel, quite conservative values), the e^{-S} term alone would cause a barrier increase of >7.5 kcal/mol (rate drop of $>3.2 \times 10^5$) for hydrazines relative to aromatics, and of >6.2 kcal/mol (rate drop $>3.6 \times 10^4$) for hydrazines relative to ferrocenes. Although these barrier increases would be halved for cross reactions, the e^{-S} dependence predicted for strongly nonadiabatic reactions is not consistent with our data. Our results are consistent with a view that intermolecular electron-transfer reactions occur in the "elbow" between adiabatic and nonadiabatic behavior, and that eqs 6 and 7 are appropriate for their analysis.

Unfortunately, there has been no good way to obtain experimental values for either H_{ab} or K_e of intermolecular reactions.[11] Eberson[12] and Kochi[13] have argued that H_{ab} is often large enough that ΔG^* is significantly smaller than $\lambda/4$, estimating that H_{ab} for unhindered aromatic systems exceeds 1

(9) Equation 7 has been slightly modified from eq 3.6 of ref 5 (p 52). Because we want to use this expression for intermolecular reactions in the H_{ab} region near adiabaticity, we include K_e and replace the $\lambda/4$ in the exponential expression by ΔG^*, which becomes significantly smaller than $\lambda/4$ as H_{ab} gets larger.

(10) Cortes, J.; Heitele, H.; Jortner, J. *J. Phys. Chem.* **1994**, *98*, 2527. For application to intramolecular thermal electron-transfer reactions, see: Nelsen, S. F.; Ramm, M. T.; Wolff, J. J.; Powell, D. R. *J. Am. Chem. Soc.* **1997**, *119*, 6863.

(11) The equations presented[2b] for calculating K_e assume without comment that $\Delta H°$ for encounter complex formation is zero. It seems likely to us, as to others,[12,13] that this assumption is often inadequate.

(12) (a) Eberson, L.; Shaik, S. S. *J. Am. Chem. Soc.* **1990**, *112*, 4484−9. (b) Eberson, L. *New J. Chem.* **1992**, *16*, 151.

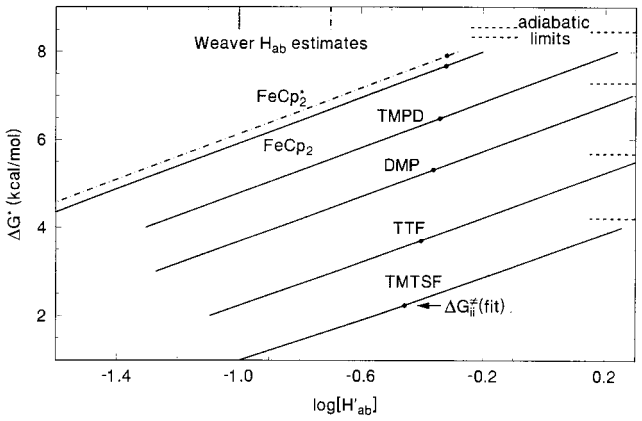

Figure 6. Plot of ΔG^* versus $\log[(K_e)^{1/2}H_{ab}]$ using eq 7 for the $\Delta G^{\ddagger}_{ii}$(fit) values of four aromatic and two ferrocene couples.

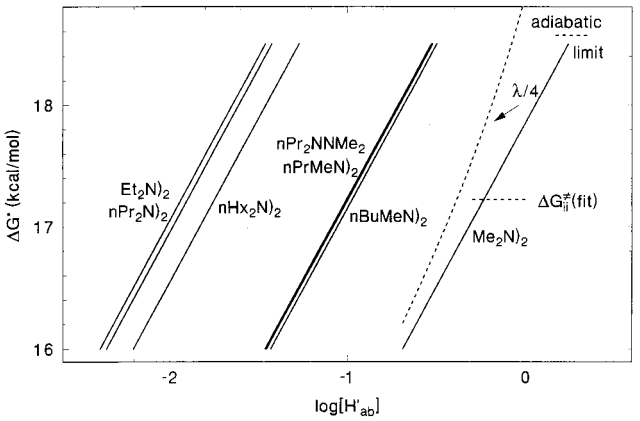

Figure 7. Plot of ΔG^* versus $\log[(K_e)^{1/2}H_{ab}]$ using eq 7 for the $\Delta G^{\ddagger}_{ii}$(fit) values of the seven methyl, *n*-alkyl hydrazines studied.

kcal/mol by considering comparison of k_{ij}(obsd) values with expectation based upon theory.[14] We note that $H_{ab} = 1$ kcal/mol is not a particularly special point on the surfaces in Figure 4. The ΔG^* value at $H_{ab} = 1$ kcal/mol is 0.5 kcal/mol smaller than the adiabatic limit (that at $\kappa_{el} = 1$, 7.65 kcal/mol for the data plotted), corresponding to a factor of 2.6 in the rate constant. The curve is so flat that it is clear that H_{ab} in this region cannot be determined accurately from an experimental rate constant. Increasing steric hindrance might be expected to lower both H_{ab} and K_e, and in the absence of being able to measure either independently, it is impossible to evaluate their individual contributions. We will therefore discuss $H'_{ab} = (K_e)^{1/2}H_{ab}$ values for the remainder of this paper.

We suggest it is instructive to consider the lowest barrier aromatic couples first. Using the L&D eq 7, each $\Delta G^{\ddagger}_{ii}$(fit) value produces a line for a ΔG^* versus $\log[(H'_{ab}]$ plot (see Figure 6). The lines have the same slope and are displaced vertically by negligibly less than $\Delta\Delta G^{\ddagger}_{ii}$(fit), so if changes in $\Delta G^{\ddagger}_{ii}$(fit) correlate with changes in ΔH_v (as in Figure 3), this implies that the H'_{ab} values for these couples are not very different, although it does not allow telling what they are. **TMPD**$^{0/+}$ is about the fastest couple for which an activation limited k_{ii}(self) can be reliably determined (faster ones develop solvent friction as well as diffusion control problems). Grampp and Jaenicke have argued for a rather small H_{ab} value for the self-exchange of **TMPD**$^+$ in acetonitrile, 0.1 kcal/mol, to be consistent with k_{ii}(self),[15] while Rauhut and Clark have calculated a value of 0.65 kcal/mol using ab initio theory.[16] The k_{ii}(self) for **TMPD**$^{0/+}$ is ca. 13-fold larger than the k_{ii}(fit) value for cross reactions with eight other partners, all of them having bulky substituents (one di-, one tri-, and six tetra-α-branched hydrazines). If the reason for the smaller k_{ii}(fit) is attributed to a change in H'_{ab}, the rate ratio corresponds to a lowering of $\log[H'_{ab}]$ by 0.56 units. The $\Delta G^{\ddagger}_{ii}$(fit) values for **FeCp$_2$**$^{0/+}$ (7.7 kcal/mol) and **FeCp*$_2$**$^{0/+}$ (7.9) are in the opposite order as their $\Delta G^{\ddagger}_{ii}$(self) values (8.0 and 7.3 kcal/mol, respectively).[17] Weaver and coworkers argue from solvent effects for H_{ab} values of 0.1 and 0.2 kcal/mol, respectively, but if this difference were applied to the H'_{ab} values, it would make ΔG^* for **FeCp*$_2$**$^{0/+}$ 1.0 kcal/mol (17%) larger than that for **FeCp$_2$**$^{0/+}$. This seems a large difference for the structural change, but the methyl groups might significantly lower K_e for **FeCp*$_2$**$^{0/+}$, compensating for a H_{ab} increase and keeping the ΔG^* values as well as the $\Delta G^{\ddagger}_{ii}$(fit) values similar.

Figure 7 shows the L&D equation interpretation of $\Delta G^{\ddagger}_{ii}$(fit) for the seven hydrazines studied that have only methyl and *n*-alkyl substituents. The least hindered couple, **(Me$_2$N)$_2$**, is shown with its adiabatic limit ΔG^*, and a dotted line showing that $\lambda/4$ becomes increasingly greater than the ΔG^* value as H'_{ab} increases. We think it quite possible that H'_{ab} for **(Me$_2$N)$_2$** could be larger than that for **TMPD**. Its π system is considerably smaller and the reactions studied include two unhindered aromatic couples (**TTF** and **TMTSF**). Because we expect very similar ΔG^* values for methyl and *n*-alkylhydrazines, we show the same ranges of ΔG^* for all seven compounds. To the extent that $\lambda_v + \lambda_s$ becomes smaller as *n*-alkyl groups replace methyl groups, using Figure 7 with constant ΔG^* would underestimate the drop in H'_{ab}. We suggest that Figure 7 makes it clear that the higher $\Delta G^{\ddagger}_{ii}$(fit) values for the compounds with more *n*-alkyl groups replacing methyl groups are caused by smaller H_{ab} values. The rather small structural changes studied here also test the reproducibility of the measurements, which appears to be rather high. The expected decrease of λ_s as effective radius of the couples increases is largely not observed (and we think the effect is overestimated using Marcus' solvent effect equation), but perhaps it contributes to the slightly smaller $\Delta G^{\ddagger}_{ii}$(fit) observed for **(^{n}Hx$_2$N)$_2$**. As pointed out previously,[6e] the N−C bond rotational preference for *n*-alkyl groups that places the β carbons alternately above and below the N,C$_\alpha$ plane ought to block close approach of a partner to the charge-bearing NN π system, rationalizing a decrease in H'_{ab}. This hypothesis is tested by the *N*,*N*-cycloalkyl compounds, which sterically preclude attaining the conformations that block approach to the nitrogens, and it may be noted from Table 1 that closing these rings indeed lowers $\Delta G^{\ddagger}_{ii}$(fit). The seven-membered ring compound **r7NNMe$_2$** is the only one with a slightly larger $\Delta G^{\ddagger}_{ii}$(fit) than **(Me$_2$N)$_2$**, and the seven-membered ring is large enough to allow partial blocking.

Although there clearly is a negative increment in H'_{ab} as methyl groups are replaced by *n*-alkyl groups, we suggest that even for **(Et$_2$N)$_2$**, ET is proceeding by the rather small overlap

(13) (a) Fukizumi, S.; Wong, C. L.; Kochi, J. K. *J. Am. Chem. Soc.* **1980**, *102*, 2928. (b) Fukizumi, S.; Kochi, J. K. *Bull. Chem. Soc. Jpn.* **1983**, *56*, 969. (c) Kochi, J. K. *Angew. Chem., Int. Ed. Engl.* **1988**, *27*, 1227. (d) Hubig, S. M.; Bockman, T. M.; Kochi, J. K. *J. Am. Chem. Soc.* **1996**, *118*, 3842. (e) Hubig, S. M.; Rathore, R.; Kochi, J. K. *J. Am. Chem. Soc.* **1999**, *121*, 617−626. (f) Hubig, S. M.; Kochi, J. K. *J. Am. Chem. Soc.* **1999**, *121*, 1688.

(14) Both Eberson and Kochi designate reactions having $H_{ab} \geq 1$ kcal/mol as being of the "inner-sphere" type, by which they appear to mean that the adiabatic version of Marcus theory that employs $\Delta G^* = \lambda/4$ does not give a large enough rate constant.

(15) Grampp, G.; Jaenicke, W. *Ber. Bunsenges. Phys. Chem.* **1991**, *95*, 904.

(16) Rauhut, G.; Clark, T. *J. Chem. Soc., Faraday Trans.* **1994**, *90*, 1783.

(17) McMannis, G. E.; Nielson, R. M.; Gochev, A.; Weaver, M. J. *J. Am. Chem. Soc.* **1989**, *111*, 5533.

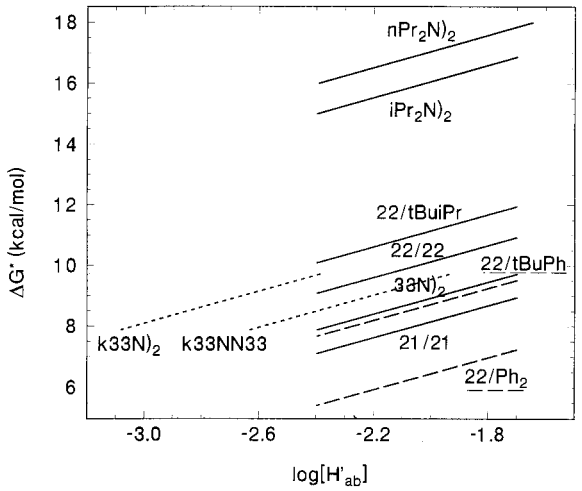

Figure 8. Plot of ΔG^* versus $\log[(K_e)^{1/2}H_{ab}]$ using eq 7 for the $\Delta G^{\ddagger}_{ii}$(fit) values of several α-branched hydrazines, compared with that for the tetra-*n*-propyl compound.

attainable by electronic interaction between nonbonded alkyl groups, suggested to be on the order of 10^{-2} kcal/mol in Figure 7. If this is true, further increasing alkyl group size by introducing α-branching should not significantly affect H_{ab}. We therefore show the data for several α-branched compounds in the same $\log[H'_{ab}]$ range as for **(^{n}Pr$_2$N)$_2$** in Figure 8. The saturated compounds (shown as solid lines) have $\Delta G^{\ddagger}_{ii}$(fit) values that reflect the changes expected in λ_v rather well, independently suggesting that their H'_{ab} values are not too different. Replacing the isopropyl group of **22/^{t}Bu^{i}Pr** by phenyl and both alkyl groups by phenyl (shown as long-dashed lines in Figure 8) probably does not change the hindrance to approach and presumably H'_{ab} very much, but significantly lowers $\Delta G^{\ddagger}_{ii}$(fit), interpreted in Figure 8 as decreasing ΔG^*. Replacing the γ-CH_2 groups of **(33N)$_2$** by carbonyl groups hardly affects the geometry at nitrogen, and we believe that it cannot significantly affect λ_v, so we have plotted **k33NN33** and **(k33N)$_2$** in Figure 8 at the same ΔG^* values as the parent with hydrocarbon substituents, to show visually how much H'_{ab} is lowered by the carbonyl substituents.

Conclusions

Equation 2 successfully correlates all k_{ij}(obsd) values we have measured, demonstrating that regardless of theoretical predictions, an $E^{\circ\prime}$ and a single k_{ii} value for each couple are sufficient to rather accurately predict intermolecular ET rate constants for a wide variety of couples. The same k_{ii}(fit) value applies whether the reaction partner is an aromatic compound, a ferrocene, or a hydrazine, demonstrating that k_{ii}(fit) is not directly proportional to e^{-S}, so the reactions cannot occur in the strongly nonadiabatic region. Effects of varying $(K_e)^{1/2}H_{ab}$ are evident, causing a 4.6 kcal/mol increase in $\Delta G^{\ddagger}_{ii}$(fit) between tetramethyl- and tetraethylhydrazine, so the reactions studied are not in the strongly adiabatic region, where k_{ij} does not depend on the size of H_{ab}. It appears that the change in $(K_e)^{1/2}H_{ab}$ damps rather rapidly for tetraalkylhydrazines, and that similar sizes probably occur for compounds with alkyl groups larger than ethyl. This work demonstrates that intermolecular ET reactions that proceed by overlap between nonbonded alkyl groups (as many of the reactions studied must) fall in the region between strongly nonadiabatic and adiabatic reactions. Available data appear to be rationalized by the Levich and Dogodnoze type eq 7 that requires neither separation of λ into its components nor knowlege of the tunneling parameter $\tilde{\nu}_v$. We suggest that this calls into question the quantitative importance of the far more complex vibronic coupling theory treatment for estimating rate constants of ET reactions that proceed in the "normal region", where driving forces are considerably less than vertical reorganization energies, that is, for most thermal ET reactions.

If varying preexponential factors Z_{ii} are written for the k_{ii} values in eq 2, as they must be for weakly nonadiabatic reactions, applying the Marcus eq 2 actually assumes that $Z_{ij} = (Z_{ii}Z_{jj})^{1/2}$. Since k_{ij} for all reactions studied are within a factor of 3.3 and 95% of them are within a factor of 2 of the experimental value, this assumption must be a good one. We do not see how this would occur unless most of the reactions studied have rather constant $(K_e)^{1/2}H_{ab}$ values (perhaps ca. 10^{-2} kcal/mol), presumably because they occur through alkyl groups in at least one component.

Acknowledgment. We thank the National Science Foundation (under CHE-9504133, to J.R.P.), the Research Corporation (RAO269 to S.F.N.), and the University of Wisconsin for partial financial support of this work and the UWEC Foundation and Kell Container Corporation for scholarship support of D.T.H. We thank Franz Neugebauer (Max Planck Institut für Medizinische Forschung, Heidelberg) for a gift of the tetraarylhydrazines.

Supporting Information Available: Intrinsic reactivity data for the couples of Scheme 3 and a listing of reactants, k_{ij}(obsd), k_{ij}(calcd), ratio, and $\Delta\Delta G^{\ddagger}_{ij}$ for the 50 reactions (PDF). This material is available free of charge via the Internet at http://pubs.acs.org.

JA993573O